Journal of Visualized Experiments

Testing Targeted Therapies in Cancer using Structural DNA Alteration Analysis and Patient-Derived Xenografts

--Manuscript Draft--

Article Type:	Invited Methods Article - Author Produced Video
Manuscript Number:	JoVE60646R4
Full Title:	Testing Targeted Therapies in Cancer using Structural DNA Alteration Analysis and Patient-Derived Xenografts
Section/Category:	JoVE Cancer Research
Keywords:	Genomic analysis, Mate-pair sequencing, Patient derived xenografts, Tumor engraftment, DNA alteration validation, Targeted therapy
Corresponding Author:	Irina V Kovtun, Ph.D. Mayo Clinic Minnesota Rochester, MN UNITED STATES
Corresponding Author's Institution:	Mayo Clinic Minnesota
Corresponding Author E-Mail:	ivkru@yahoo.com
Order of Authors:	Irina V Kovtun, Ph.D.
	Piyan Zhang
Additional Information:	
Question	**Response**
Please indicate whether this article will be Standard Access or Open Access.	Standard Access (US$1200)

TITLE:

Testing Targeted Therapies in Cancer using Structural DNA Alteration Analysis and Patient-Derived Xenografts

AUTHORS AND AFFILIATIONS:

Piyan Zhang[1], Irina V. Kovtun[1,2]

[1]Center for Individualized Medicine Mayo Clinic, Rochester, Minnesota

[2]Department of Molecular Pharmacology and Experimental Therapeutics, Mayo Clinic, Rochester, Minnesota

Corresponding Author:

Irina V. Kovtun (ivkru@yahoo.com)

Email Address of Co-author

Piyan Zhang (pzhang3@bidmc.harvard.edu)

KEYWORDS:

Genomic analysis, Mate-pair sequencing, Patient derived xenografts, Tumor engraftment, DNA alteration validation, Targeted therapy

SUMMARY

Here we present a protocol to test the efficacy of targeted therapies selected based on the genomic makeup of a tumor. The protocol describes identification and validation of structural DNA rearrangements, engraftment of patients' tumors into mice and testing responses to corresponding drugs.

ABSTRACT

We present here an integrative approach for testing efficacy of targeted therapies that combines the next generation sequencing technologies, therapeutic target analyses and drug response monitoring using patient derived xenografts (PDX). This strategy was validated using ovarian tumors as an example. The mate-pair next generation sequencing (MPseq) protocol was used to identify structural alterations and followed by analysis of potentially targetable alterations. Human tumors grown in immunocompromised mice were treated with drugs selected based on the genomic analyses. Results demonstrated a good correlation between the predicted and the observed responses in the PDX model. The presented approach can be used to test the efficacy of combination treatments and aid personalized treatment for patients with recurrent cancer, specifically in cases when standard therapy fails and there is a need to use drugs off label.

INTRODUCTION

Patient-derived xenografts (PDXs), which are generated from the implantation of patient tumor pieces into immunodeficient mice, have emerged as a powerful preclinical model to aid personalized anti-cancer care. PDX models have been successfully developed for a variety of human malignancies. These include breast and ovarian cancers, malignant melanoma, colorectal

cancer, pancreatic adenocarcinoma, and non-small cell lung cancer[1-5]. Tumor tissue can be implanted orthotopically or heterotopically. The former, considered more accurate but technically difficult, involves transplantation directly into the organ of tumor origin. These types of models are believed to precisely mimic histology of the original tumor due to the "natural' microenvironment for the tumor[6,7]. For example, orthotopic transplantation into the bursa of the mouse ovary resulted in tumor dissemination into the peritoneal cavity and the production of ascites, typical of ovarian cancer[8]. Similarly, injection of breast tumors into the thoracic instead of the abdominal mammary gland affected the PDX success rate and behavior[9]. However, orthotopic models require sophisticated imaging systems to monitor tumor growth. Heterotopic implantation of solid tumor is typically performed by implanting tissue into the subcutaneous flank of a mouse which allows for easier monitoring of tumor growth and is less expensive and time consuming[7]. However, tumors grown subcutaneously rarely metastasize unlike as observed in the case of orthotopic implantation[10].

The success rate of engraftment has been shown to vary and greatly depend on the tumor type. More aggressive tumors and tissue specimens containing a higher percent of tumor cells were reported to have better success rates[12,13]. Consistent with this, tumors derived from metastatic sites were shown to engraft at frequencies of 50–80%, while those from primary sites engraft at frequencies as low as 14%[12]. In contrast, tissue containing necrotic cells and fewer viable tumor cells engraft poorly. Tumor growth can also be promoted by the addition of basement membrane matrix proteins into the tissue mix at the time of the injection into mice[14] without compromising properties of the original tumor. The size and number of tissue pieces intended for implantation were also found to affect the success rate of engraftment. Greater tumor take-rates were reported for implantation in the sub-renal capsule compared to subcutaneous implantation due to the ability of the sub-renal capsule to maintain the original tumor stroma and provide the host stromal cells as well[15].

Most studies use NOD/SCID immunodeficient mice, which lack natural killer cells[16] and have been shown to increase the tumor engraftment, growth and metastasis compared to other strains[14]. However, additional monitoring is required as they may develop thymic lymphomas as early as 3-4 month of age[13]. In ovarian tumor transplants grown in SCID mice, the outgrowth of B cells was successfully inhibited by rituximab, preventing the development of lymphomas but without impacting the engraftment of ovarian tumors[17].

More recently, NSG (NOD.Cg-*Prkdc*^{scid} *Il2rg*^{tm1Wjl}/SzJ) mice, carrying a null mutation in the gene encoding the interleukin 2 receptor gamma chain[18], became a frequently used strain for the generation of PDX models. Tumors from established PDX models passaged to future generations of mice are reported to retain histological and molecular properties for 3 to 6 generations[19,20]. Numerous studies have shown that the treatment outcomes in PDX models mimic those of their corresponding patients[2-4,21-23]. The response rate to chemotherapy in PDX models for non-small lung cancer and colorectal carcinomas was similar to that in clinical trials for the same drugs[24,25]. Studies conducted in PDX models, developed for patients enrolled in clinical trials, demonstrated responses to tested drugs similar to those observed clinically in corresponding patients[2-4].

High–throughput genomic analyses of a patient tumor in conjunction with PDX models provide a powerful tool to study correlations between specific genomic alterations and a therapeutic response. These have been described in a few publications[26,27]. For example, therapeutic responses to the EGFR inhibitor cetuximab in a set of colorectal PDX models carrying EGFR amplification, paralleled clinical responses to cetuximab in patients[28].

There are a few challenges associated with the development and application of PDX models. Among those is tumor heterogeneity[29,30] that may compromise the accuracy of treatment response interpretation as a single cell clone with higher proliferative capacity within a PDX can outgrow the other ones[31], thus resulting in a loss of heterogeneity. Additionally, when single tumor biopsies are used to develop PDX, some of the cell populations may be missed and will not be represented in the final graft. Multiple samples from the same tumor are recommended for implantation to resolve this issue. Although PDX tumors tend to contain all the cell types of the original donor tumor, these cells are gradually substituted by those of murine origin[3]. The interplay between murine stroma and human tumor cells in PDX models is not well understood. Nevertheless, stromal cells were shown to recapitulate tumor microenvironment[33].

Despite these limitations, PDX models remain among the most valuable tools for translational research as well as personalized medicine for selecting patient therapies. Major applications of PDXs include biomarker discovery and drug testing. PDX models are also successfully used to study drug resistance mechanisms and identify strategies to overcome drug resistance[34,35]. The approach described in the present manuscript allows the researcher to identify potential therapeutic targets in human tumors and to assess the efficacy of corresponding drugs in vivo, in mice harboring engrafted tumors which were initially genomically characterized. The protocol uses ovarian tumors engrafted intraperitoneally but is applicable to any type of tumor sufficiently aggressive to grow in mice[2,3,12].

PROTOCOL

Fresh tissues from consenting patients with ovarian cancer were collected at the time of debulking surgery according to a protocol approved by Mayo Clinic Institutional Review Board (IRB). All animal procedures and treatments used in this protocol were approved by Mayo Clinic Institutional Animal Care and Use Committee (IACUC) and followed animal care guidelines.

1. Mate pair sequencing and analyses

NOTE: Either fresh or flash frozen tissue must be used for mate pair (MPseq) sequencing. Paraffin embedded material is not suitable because it contains fragmented DNA.

1.1. Isolate DNA from frozen tumor tissue. Use original human specimen obtained from surgical material or biopsy[36].

1.2. Use 1000 ng of DNA to make MPseq libraries and sequence as 2 samples per lane on the next generation sequencer (see **Table of Materials**)[36].

1.3. Analyze data using a set of algorithms to detect large chromosomal aberrations (deletions, insertions, amplifications, inversions and translocations) as described earlier[36,37].

2. Selection of therapeutic targets

2.1. Use the open access Panda tool (Pathway and Annotation) or an analogous tool to identify targetable alterations (http://bioinformaticstools.mayo.edu/Panda).

2.1.1. Make a list of genes that are identified by MSeq as altered, as a simple tab-delimited file, using standard accepted gene symbols.

NOTE: The included example features analysis of amplifications and gains.

2.1.2. Add a "#" sign to the header line of the list to ensure that the table header is transferred to the pathway level view of the software.

2.1.3. Upload the file by clicking the **Upload Annotation Set** navigation tab.

2.1.4. Assign a single icon from the menu to represent the underlying data by clicking on the icon of choice and then clicking the **Finalize** tab.

2.1.5. After the annotation files are uploaded, identify a column that displays the number of annotated genes per pathway. This is the last column on the right.

2.1.6. Use **Pathway Filter** on the upper left of the main window to show pathways containing genes of interest.

2.1.7. Identify pathways that have more annotated genes than is expected by chance. Use the function located under the **Enrichment** tab.

2.1.8. Select a database to display potentially druggable genes from **Preset Annotation** by checking an appropriate icon on the left of the main window (e.g., DGIdb, PharmGKB).

2.1.9. Select pathway for visualization by clicking on its name displayed in the **Pathway Viewer** page.

NOTE: Icons representing each annotation set are shown next to the associated gene. Click on the gene of interest to open the corresponding GeneCards webpage.

2.1.10. Select the pathways that showed the annotated genes of interest (i.e., altered in a given tumor) and "hits" for potential drugs for further analysis.

2.2. Use a database containing drugs approved for clinical application (https://clinicaltrials.gov/) to cross-reference the identified targets.

2.3. Prioritize targetable alterations for further testing in PDX models by performing a literature review (e.g., PubMed) to confirm relevance to the biology of a particular type of tumor.

3. Validation of genomic rearrangements by PCR and Sanger sequencing

3.1. Design primers using sequencing reads obtained from MPseq data.

3.1.1. Select a junction of interest for the validation (i.e., potential therapeutic target) based on MPseq analyses.

3.1.2. Design primers directionally such that the amplicon contains the junction. Design 2 primers on each side of the junction, for a total of 4, to increase the chances of amplifying the junction.

NOTE: Name primers according to the case and chromosome location.

3.1.3. Use standard PCR parameters for the primer design and a software of choice. Select melting temperature (60-62 ˚C) and the GC content (40-60%). Make sure that the primer sequence does not form primer dimers, palindromes or hairpin loops.

3.1.4. Confirm that the primer sequence lacks homology to other areas of the human genome by checking it using BLAT (http://genome.ucsc.edu/cgi-bin/hgBlat?command=start).

3.2. Run a PCR to amplify the junction of interest.

3.2.1. Dilute primers with water to 10 mM and combine 10 µL of each primer so that each forward primer is paired with each reverse primer into a primer mix.

NOTE: Sequences for the primers for the selected example are shown in **Table 1**.

3.2.2. Label 0.2 mL strip tubes as: C1, T1, C2, T2, C3, T3, C4 and T4 where C=control human genomic DNA (commercial), T=Tumor DNA, isolated from patient or PDX tumor, and the number indicates the primer mix.

3.2.3. Add 1 µL of each primer mix into its labeled tubes.

3.2.4. Prepare the Taq mastermix by combining reagents listed in **Table 2**, leaving the enzyme in the freezer until needed, adding it to the mix at the very end.

3.2.5. Make 2 master mixes, one for each template DNA, control human DNA and tumor DNA. Add 24 μL of each Taq master mix to its respective strip tube. The total reaction volume is 25 μL. Vortex very briefly and then spin the strip tube down.

3.2.6. Run a PCR in a thermocycler. Use the parameters shown in **Table 3.** Adjust the annealing temperature so that it is at least 1 °C colder than the melting temperature of the primers.

3.2.7. Store the completed PCR product at -20 °C (long term) or refrigerated at 4 °C (short term) until needed.

3.2.8. Perform electrophoresis at 1-5 V/cm to visualize PCR product using a 1.5% agarose gel. Leave 2 mL aliquot of the product to be used for Sanger sequencing.

3.3. Perform Sanger sequencing to confirm the junction and identify the exact breakpoint[38].

3.3.1. Use the PCR product if the PCR generated a single product (band). Alternatively, cut the band out of gel, purify and submit for Sanger sequencing along with the primer used for amplification.

NOTE: The tumors for which genomic analyses were performed then are used for implantation in mice.

4. Tumor engraftment and maintenance

4.1. Set up preparations to engraft tumors into PDX mouse models. Select for engraftment tumors for which genomic analyses will be or has been performed.

4.1.1. Make sure that a supportive infrastructure is in place at the time of the start of the development of any PDX models, including dedicated laboratory and animal facilities, skilled technical staff and detailed standard operating procedures.

4.1.2. Ensure the quick transportation and processing of specimens as speed is crucial for cell viability and successful engraftment.

4.1.3. Use a sterile environment to reduce bacterial and fungal contamination for processing and engrafting specimens.

4.1.4. Handle human specimens with caution, in accordance with institutional policies regarding potentially biohazardous materials, as they may harbor blood-borne pathogens.

4.1.5. Prepare the tissue (0.5-0.7 cm^3 in size) for engraftment by putting the surgical specimen into a pre-chilled 50 mL tube with 20 mL of tissue culture media.

NOTE: The tumor tissue can be fresh or recovered from previously cryopreserved material[5].

4.1.6. Confirm the tumor content in the specimen by consulting a pathologist.

4.1.7. Place the tumor tissue in a dish containing 10-15 mL of cold PBS, or tissue culture media such as RPMI 1640 or DMEM containing antibiotics (1% penicillin and streptomycin).

4.1.8. Identify and isolate viable tumor material from adjacent normal and necrotic tissue with the help from a pathologist. Use sterile forceps and scalpel to remove necrotic material pointed out by a pathologist.

NOTE: The tumor can be implanted either intraperitoneally or subcutaneously into the mice. Follow step 4.2 to perform an intraperitoneal implantation or skip to step 4.3 to perform a subcutaneous engraftment. In this study, targeted therapies selected based on genomic analyses were tested in a series of PDX models for high grade serous ovarian cancer with intraperitoneal implantation.

4.2. Prepare the tissue for intraperitoneal (IP) implantation mincing the tissue with sterile forceps and a scalpel on ice to make pieces approximately 1-1.5 mm^3 in size and mixing with cold culture medium. Inject 0.3–0.5 mL of tumor slurry using a 16-17 gauge needle.

NOTE: All surgical procedures are performed by using aseptic techniques. Sterile gloves, sterile instruments, supplies, and implanted materials were used to reduce the likelihood of infection.

4.2.1. Mix the pieces 1:1 with ice-cold culture medium and inject 100 mL intraperitoneally in at least three female SCID mice.

4.3. Cut the tumor tissue for subcutaneous engraftment using sterile forceps, scalpel, or surgical scissors into small fragments, roughly 2 x 2 x 2 mm in size, and transfer the fragmented tissues to a pre-chilled Petri dish on ice.

4.3.1. Add the cold basement membrane matrix into the dish with the fragmented tissue (approximately 200 mL per 10 pieces of tissue), mix well, and let the tissue fragments soak in the cold basement membrane matrix for 10 min.

4.3.2. Anesthetize 5 female NOD/SCID mice to prepare them for engraftment.

4.3.3. Inject each mouse intraperitoneally with ketamine (150 mg/kg) and xylazine (10 mg/kg) combination.

4.3.4. Confirm that mouse is properly anesthetized by pinching the tail tip with atraumatic forceps.

4.3.5. Remove gently fully anesthetized mouse from the chamber and put on the mouse a nose cone which has input from vaporizer and output from waste gas scavenging system.

4.3.6. Put vet ointment on mouse eyes to prevent dryness while under anesthesia. Prepare the area where the surgery will be performed. Use aseptic technique to perform the surgery.

4.3.7. Ensure that the surface on which the surgery is going to take is non-porous, sealed and is disinfected prior to surgery.

4.3.8. Start surgery with sterile (by autoclave, gas or chemical sterilization) instruments.

4.3.9. Use gloves to handle instruments and maintain the sterility of the instrument tips throughout the procedure by submerging them in ethanol between surgery steps.

4.4. Sterilize the surgical site by applying 3 alternating scrubs of iodine and alcohol. Use sterile surgical scissors and forceps to make a 5-10 mm vertical skin incision on both flanks of a mouse.

4.4.1. Insert straight forceps gently into the subcutaneous space to create a pocket large enough for a tumor fragment to be placed under the fat pad.

4.4.2. Use the sterile straight forceps to insert tumor fragments into previously prepared pocket in each of 5 mice.

NOTE: Place 3-4 pieces of tumor tissue in one pocket.

4.4.2. Close the skin incisions using tissue glue.

4.4.3. Intraperitoneally inject each mouse with 100 mL of Rituximab after implantation to inhibit lymphocyte proliferation.

4.5. Place the mouse into a cage under a heat lamp for approximately 20 min until recovered from anesthesia. Monitor the mouse vital signs and ensure its sufficient hydration.

4.6. Return the mouse to the company of other mice after it recovered from anesthesia and started to have food and water. Provide postoperative care and monitoring according to institutional guidelines. Check for signs of pain and distress daily for 3 consecutive days after surgery.

NOTE: Criteria for pain or distress include necrosis or ulceration, weight loss/body condition scoring, behavioral signs such as activity level, motor function and posture.

4.7. Routinely check the mice for tumor formation bi-weekly until the tumors reach the size of 0.5 cm in diameter as measured by a caliper.

4.8. Assess the health score of each mouse as derived from appearance, behavior, and body condition[39]. Use scores of ≤6 as criteria for moribund mice to be sacrificed by carbon dioxide inhalation.

5. Testing responses to genomically identified targets in PDX models

5.1. Start the selected targeted treatments when the tumors are palpable and reach 0.5 cm^3 as measured by an ultrasound scan.

5.1.1. Prior to performing an ultrasound scan of the abdomen remove the mouse abdominal fur and apply sterile jelly lubricant.

5.1.2. Use an ultrasound machine with a transducer to obtain images with the tumor positioned in cross-section. Make 3 measurements per session for each animal and average the value for a more accurate assessment of tumor size.

5.1.3. Analyze the images using available software[40].

5.2. Administer chemotherapy consisting of a mixture of carboplatin at 51 mg/kg and paclitaxel at 15 mg/kg intraperitoneally (IP) once a week for a total treatment duration of 4-6 weeks. Make sure that total volume for injection does not exceed 0.2 mL.

5.3. Make a MK-2206[41] stock solution in 30% cyclodextrin (e.g., Captisol) and deliver via oral gavage at 120 mg/kg daily for 4 consecutive weeks.

5.4. Prepare the mouse for oral gavage by hold it by pinching the skin of the back and pinning it back, so that the head and limbs of the mouse are immobilized.

5.4.1. Insert the gavage probe down the back of the throat of the mouse until the probe reaches the esophagus. Make sure that the probe is not inserted too far, as the lungs of the mouse may perforate, causing death.

5.5. Make a MK-8669[42] stock solution in ethanol at 25 mg/mL. Dilute it in a vehicle containing 5.2% Tween 80, 5.2% PEG400 in sterile water for IP injections at 10 mg/kg for 5 days every other week, with a total duration of the treatment of 4 weeks.

NOTE: Volume injected into mice should be 50-120 mL, depending on animal's weight.

5.6. Use 7-8 mice per treatment group to have enough statistical power to detect differences[43,44].

5.7. Assess body weight and general condition of the mice in therapy daily. Withhold drugs if an animal's weight drops 20% or more from their initial weight.

5.7. Assess the tumor size weekly by using ultrasound scanning. Make sure that the individual performing the monitoring of the tumor growth is blinded to the treatment to ensure the unbiased scoring of responses.

NOTE: Smaller laboratories may employ 2 different people to administer treatment and ultrasound monitoring.

REPRESENTATIVE RESULTS

Tissue from resected ovarian tumors at the time of debulking surgeries were collected in accordance with IRB guidance and used for 1) genomic characterization and 2) engraftment in immunocompromised mice (**Figure 1**). Mate-pair sequencing protocol[36,37] was used to identify structural alterations in DNA including losses, gains and amplifications. A representative genome plot illustrating a landscape of genomic changes in one tumor (designated as OC101) is shown in **Figure 2**. Typical for high grade serous subtype tumors, multiple gains (blue lines) and deletions (red lines) were found, indicating high levels of genomic instability, as well as chromosomal losses and gains, indicative of aneuploidy, were observed. On an average 300-700 alterations total are identified in high grade serous subtype tumors[45]. Subsequent analyses revealed a few DNA alterations that were potentially targetable with clinically relevant drugs. The top-ranked alteration for therapeutic intervention in the OC101 tumor was an amplification at chromosome 17 involving ERBB2 (**Figure 2** and **Figure 3A**). ERBB2 is a gene which codes for HER2 receptor which is known upon dimerization with EGFR, HER3 or HER4 to activate RAS/ERK and PI3K/AKT signaling pathways and promote cell growth, cell migration and invasion. HER2 inhibitors (e.g., monoclonal antibodies pertuzumab and trastuzumab) are effective in treating breast cancer patients when tumors overexpress the HER2 protein. Anti-HER2 therapy for ovarian cancer, however, is not FDA approved.

Comparison of the genomic profile of donor patients' tumor (**Figure 1**) to that of a corresponding PDX model (not shown) revealed a striking similarity, consistent with all previous studies reporting the molecular closeness of original tumors to their PDX derivatives.

To validate MPseq results at the DNA level, several sets of specific primers were designed for the edges of amplified region containing the ERBB2 gene, and PCR was carried out using DNA isolated from the original tumor as well as from a tumor propagated for several generations in the mice. A representative gel image of amplified products using two different sets of primers is shown in **Figure 3B**. No band was detected when normal pooled genomic DNA (designated as C), that did not contain amplification of the ERBB locus, was amplified. Purification of the products from the gel and Sanger sequencing (not shown) further confirmed the alteration predicted by MPseq. Further validation was conducted by examining the expression of HER2 protein in the corresponding PDX tumor using immunoblotting. The analysis revealed a high level of HER2 protein (the result is not shown), consistent with the observed amplification of the ERBB2 gene.

In the DNA of a different ovarian tumor (designated T14) numerous regional gains were observed. Those included AKT2 and RICTOR genes (**Figure 3C**). Both were of great interest from a therapeutic perspective as inhibitors of AKT2 and mTOR, which RICTOR associates with, are

available and currently in clinical trials. Since there were no mate pair reads spanning the vicinity of either gene, simple PCR validation of the gain as detected by MPseq was not possible. We, therefore, tested the expression level of corresponding proteins by immunoblotting. High levels of AKT and RICTOR were observed (**Figure 3D**) suggesting that treatment with targeted drugs is warranted.

To test the sensitivity of this tumor to inhibitors of AKT and mTOR, PDX mice with intraperitoneally implanted T14 tumor were expanded and randomized to receive only chemotherapy (carboplatin/paclitaxel) or a combination of chemotherapy with pan-AKT inhibitor MK-2206[41] or mTOR inhibitor MK-8669[42]. Chemotherapy was given to mice in the combination arm for 2 weeks prior to the addition of the targeted therapy (**Figure 4**). Ultrasound measurements were taken weekly to monitor tumor regression/growth.

Each treatment arm contained no less than 7 mice. This number was sufficient to observe differences in responses between the groups while keeping costs of the study at a considerably lower mark. Fewer mice (three to four) can be used in the control untreated group, as individual variations in tumor growth rate are negligible and growth is normalized to a tumor size at which treatment in other arms begins.

No difference was observed between chemo-treated and untreated groups in the first 3 weeks of observation (not shown). A significant reduction of tumor burden (58% median) was observed in the chemotherapy treated group by the end of week 6. An extra benefit over chemotherapy alone was observed in groups which received a combination of chemotherapy with targeted therapies. The difference became evident at week 4 and 3 for MK-8669 (Figure 4A) and MK-2206 (**Figure 4B**) respectively.

Animals were euthanized and tumor tissue was collected for molecular analyses of treatment response at the end of the treatment trial at week 7. For that purpose the amounts of total and phosphorylated S6 kinase (**Figure 5A**,**B**), AKT and mTOR (**Figure 5C**,**D**) were determined using immunoblotting. Ribosomal protein S6 kinase is a downstream messenger of the AKT-mTOR pathway, known to be up-regulated and phosphorylated upon stimulation of the AKT-mTOR axis by growth factors to promote cell survival and growth. Comparison of the levels of these proteins in untreated or treated with chemotherapy PDX tumors to mice that received AKT or mTOR inhibitors showed a marked decrease in the latter two (**Figure 5**), indicating effectiveness of the targeted therapy on the molecular level. Adjustments to the treatment regiment, as far as application timing for the combined drugs and therapy duration, should be made and tested to achieve better responses.

Table 1. Primers used for the validation of the OC101chromosome 17 alteration.

Table 2. PCR setup to validate a junction.

Table 3. Cycling conditions for PCR to validate a junction.

Figure 1: Schematic representation of the strategy for genomically-guided therapy testing using PDX models for serous ovarian carcinoma. H&E staining of ovarian tumor is shown (top). Scale bar=100 mm.

Figure 2: Genomic characterization of ovarian tumors using MPseq. Genome plot showing the landscape of structural alterations and copy number changes as detected by MPseq. The X axis spans the length of the chromosome with chromosome position number shown. Each chromosome is indicated on the right and left Y-axis. The height of the horizontal traces for each chromosome indicates the number of reads detected for 30k base pair windows. DNA copy numbers are indicated by color, with grey representing the normal 2N copy state, red corresponding to deletions and blue-to gains. Connecting black lines correspond to chromosomal rearrangements. Alterations at ERBB2 locus are depicted.

Figure 3: Selection of targetable alterations and their validation. (**A**) A close-up segment of the genome plot shown in Fig.1 illustrating an amplification of the ERBB2 gene on chromosome 17 (in blue). Chromosome numbers are as indicated. (**B**) Validation analysis of breakpoints at ERBB2 locus as identified by MPseq using PCR amplification. C is a pooled genomic DNA control, OC101 is DNA from patient tumor, M is a DNA ladder. (**C**) A close-up of segments of the genome plot for another ovarian tumor showing gains (indicated by blue line) at the AKT locus (top) and at the RICTOR gene (bottom). Chromosomes are as indicated. (**D**) Validation analysis of expression of proteins of AKT/mTOR pathway by immunoblotting using tumor tissue from PDX (T14), genomic alterations for which are depicted in C. 30 mg of total protein and specific antibodies to AKT, RICTOR, p-mTOR were used. MAPK served as a loading control. Pos con is an independent tumor used as a positive control.

Figure 4: The comparison of responses to chemotherapy alone and combined with targeted therapy in tumor harboring gains at AKT2 and RICTOR genes with corresponding drugs. Treatment responses to a combination of chemotherapy and anti-mTOR drug MK-8669 (**A**) or inhibitor of pan-AKT MK2206 (**B**) versus chemotherapy alone. The time of administration for each treatment and the duration are shown by the arrows. Volumes are expressed as percent of initial volume at the start of the treatment as mean +/- SD. Chemo is chemotherapy.

Figure 5: Comparison of molecular changes elicited by each treatment as determined by immunoblotting analysis. (**A**) Levels of S6 and phospho-S6, the downstream effector of AKT-mTOR pathway are shown. 30 mg of total protein and specific antibody to S6 and p-S6 were used. GAPDH was used as a loading control. Quantification of protein levels normalized to GAPDH level is shown in (**B**) (**C**) Levels of mTOR, p-mTOR, AKT and p-AKT as detected by immunoblotting. GAPDH was used as a loading control. (**D**) Quantification of protein levels normalized to GAPDH level. NT is not treated, chemo is chemotherapy.

DISCUSSION

We describe the approach and protocols we used to conduct a “clinical trial” in PDX models that takes advantage of molecular characteristics of the tumor as obtained by genomic profiling to determine the best choice of drugs for testing. Multiple sequencing platforms are currently used

for genomic characterization of primary tumors including whole genome sequencing, RNAseq and customized gene panels. For high grade serous ovarian carcinoma, MPseq to identify structural alterations, DNA rearrangements and copy number changes, is particularly useful because of the high degree of genomic instability observed in this type of tumor. The second advantage of the MPseq platform is that it covers the entire genome but costs significantly less than other comprehensive sequencing technologies. MPseq, however, is not suitable for point mutation detection as base coverage is not sufficient, reaching only 8-10x. One of the limitations of using MPseq alone for genomic characterization of a tumor is the presence of complex clustered chromosomal rearrangements, analysis of which does not predict the expression of impacted genes of interest. A junction detected by MPseq predicted to create a putative fusion gene that validates in the DNA by PCR may not be expressed because of a frame shift or small deletions and insertions in the promoter region. Similarly, chromosomal gains and amplifications for potential therapeutic targets should be carefully assessed and validated on the RNA or protein level to ensure expression of the gene of interest.

Although, the molecular make-up of the tumor is largely preserved after propagation in mice for several generations, changes in expression levels of key genes may occur over time either reflecting tumor evolution, clonal selection or adaptive response to murine environment. Thus, validation of an alteration intended for therapeutic intervention in both original donor tumor and PDX tumor is critical. For tumor isolated from PDX models both RNA and protein can be used to interrogate the expression level as the material is abundant. Either one can be chosen to cross-check the expression in the original tumor, depending on the availability and type of the stored tissue, and availability of antibody for the corresponding protein detection. The PDX model is specifically invaluable in testing combination therapies as the in vivo setting allows the monitoring of adverse effects, as well as dosage or duration adjustments in the treatment regimen.

The choice between orthotopic and subcutaneous engraftment can be made depending on the specific questions being addressed in the study. However, it is important to keep in mind that the sensitivity of xenografted tumors to therapeutics may be modulated by the site of implantation[46]. On the other hand, no evidence has been reported yet on the discovery of drugs showing a therapeutic response in orthotopic models but absent in subcutaneously implanted PDX[9].

ACKNOWLEDGMENTS

We thank the members of the Mayo Clinic Center for Individualized Medicine (CIM) Dr. Lin Yang and Faye R. Harris, MS, for the help in conducting experiments. This work was supported by Mr. and Mrs. Neil E. Eckles' Gift to the Mayo Clinic Center for Individualized Medicine (CIM).

DISCLOSURES:

The authors declare that they have no conflict of interest.

REFERENCES

1. Tentler, J.J. et al. Patient-derived tumour xenografts as models for oncology drug development. *Nature Reviews Clinical Oncology.* **9**, 338-350 (2012).

2. Marangoni, E. et al. A new model of patient tumor-derived breast cancer xenografts for preclinical assays. *Clinical Cancer Research.* **13**, 3989-3998 (2007).
3. Zhang, X. et al. A renewable tissue resource of phenotypically stable, biologically and ethnically diverse, patient-derived human breast cancer xenograft models. *Cancer Research*. **73**, 4885–4897 (2013).
4. Hidalgo, M. et al. Patient-derived xenograft models: an emerging platform for translational cancer research. *Cancer Discovery*. **4**, 998–1013 (2014).
5. Weroha, S.J. et al. Tumorgrafts as in vivo surrogates for women with ovarian cancer. *Clinical Cancer Research.* **20**, 1288-1297 (2014).
6. Rubio-Viqueira, B. et al. Optimizing the development of targeted agents in pancreatic cancer: tumor fine-needle aspiration biopsy as a platform for novel prospective ex vivo drug sensitivity assays. *Molecular Cancer Therapeutics.* **6**, 1079-1088 (2007).
7. Rubio-Viqueira, B, Hidalgo, M. Direct in vivo xenograft tumor model for predicting chemotherapeutic drug response in cancer patients. *Clinical Pharmacology and Therapeutics.* **85**, 217–221 (2009).
8. Ricci, F. et al. Patient-derived ovarian tumor xenografts recapitulate human clinicopathology and genetic alterations. *Cancer Research.* **74**, 6980-6990 (2014).
9. Fleming, J.M. et al. Local regulation of human breast xenograft models. *Journal of Cellular Physiology.* **224**, 795–806 (2010).
10. Hoffman, R.M. Patient-derived orthotopic xenografts: better mimic of metastasis than subcutaneous xenografts. *Nature Reviews Cancer.* **15**, 451-452 (2015).
11. Jung, J., Seol, H.S., Chang, S. The Generation and Application of Patient-Derived Xenograft Model for Cancer Research. *Cancer Research and Treatment.* **50**, 1-10 (2018).
12. Sivanand, S. et al. *A validated tumorgraft model reveals activity of dovitinib against renal cell carcinoma. Science Translational Medicine.* **4**, 137-152 (2012).
13. Pavía-Jiménez, A, Tcheuyap, V.T., Brugarolas, J. Establishing a human renal cell carcinoma tumorgraft platform for preclinical drug testing. *Nature Protocols.* **9**, 1848-1859 (2014).
14. Fridman, R., Benton, G., Aranoutova, I., Kleinman, H.K., Bonfil, R.D. Increased initiation and growth of tumor cell lines, cancer stem cells and biopsy material in mice using basement membrane matrix protein (Cultrex or Matrigel) co-injection. *Nature Protocols.* **7**, 1138-1144 (2012).
15. Cutz, J.C. et al. Establishment in severe combined immunodeficiency mice of subrenal capsule xenografts and transplantable tumor lines from a variety of primary human lung cancers: potential models for studying tumor progression-related changes. *Clinical Cancer Research.* **12**, 4043–4054 (2006).
16. Siolas, D., Hannon, G.J. Patient-derived tumor xenografts: transforming clinical samples into mouse models. *Cancer Research.* **73**, 5315–5319 (2013).
17. Butler, K.A. et al. Prevention of Human Lymphoproliferative Tumor Formation in Ovarian Cancer Patient-Derived Xenografts. *Neoplasia.* **19**, 628-636 (2017).
18. Cao, X. et al. Defective lymphoid development in mice lacking expression of the common cytokine receptor gamma chain. *Immunity.* **2**, 223–238 (1995).
19. Dobbin, Z.C. et al. Using heterogeneity of the patient-derived xenograft model to identify the chemoresistant population in ovarian cancer. *Oncotarget.* **5**, 8750–8764 (2014).

20. Choi, Y.Y. et al. Establishment and characterisation of patient-derived xenografts as paraclinical models for gastric cancer. Scientific Reports. **6**, 22172 (2016).
21. Malaney, P., Nicosia, S.V., Davé, V. One mouse, one patient paradigm: New avatars of personalized cancer therapy. *Cancer Letters.* **344**, 1-12 (2014).
22. Rosfjord, E., Lucas, J., Li, G., Gerber, H.P. Advances in patient-derived tumor xenografts: from target identification to predicting clinical response rates in oncology. *Biochemical Pharmacology.* **91**, 135-43 (2014).
23. Braekeveldt, N., Bexell, D. Patient-derived xenografts as preclinical neuroblastoma models. *Cell and Tissue Research.* **372**, 233-243 (2018).
24. `Perez-Soler, R. et al. Response and determinants of sensitivity to paclitaxel in human non-small cell lung cancer tumors heterotransplanted in nude mice. *Clinical Cancer Research.* **6**, 4932–4938 (2000).
25. Fichtner, I. et al. Anticancer drug response and expression of molecular markers in early-passage xenotransplanted colon carcinomas. *European Journal of Cancer* **40**, 298–307 (2004).
26. Gao, H. et al. High-throughput screening using patient-derived tumor xenografts to predict clinical trial drug response. *Nature Medicine.* **21**, 1318-25 (2015).
27. Izumchenko, E. et al. Patient-derived xenografts effectively capture responses to oncology therapy in a heterogeneous cohort of patients with solid tumors. *Annals of Oncology.* **28**, 2595-2605 (2017).
28. Bertotti, A. et al. A molecularly annotated platform of patient-derived xenografts ("xenopatients") identifies HER2 as an effective therapeutic target in cetuximab-resistant colorectal cancer**.** *Cancer Discovery.* **1**, 508-23 (2011).
29. Mengelbier, L.H. et al. Intratumoral genome diversity parallels progression and predicts outcome in pediatric cancer. *Nature Communications.* **27**, 6125 (2015).
30. McGranahan, N., Swanton, C. Clonal Heterogeneity and Tumor Evolution: Past, Present, and the Future. *Cell.* **168**, 613-628 (2017).
31. Marusyk, A. et al. Non-cell-autonomous driving of tumour growth supports sub-clonal heterogeneity. *Nature.* **514**, 54–8 (2014).
32. Braekeveldt, N. et al. Neuroblastoma patient-derived orthotopic xenografts reflect the microenvironmental hallmarks of aggressive patient tumours. *Cancer Letters.* **375**, 384-389 (2016).
33. DeRose, Y.S. et al. Tumor grafts derived from women with breast cancer authentically reflect tumor pathology, growth, metastasis and disease outcomes. *Nature Medicine.* **17**, 1514-1520 (2011).
34. Das Thakur, M. et al. Modelling vemurafenib resistance in melanoma reveals a strategy to forestall drug resistance. *Nature.* **494**, 251-255 (2013).
35. Girotti, M.R. et al. Application of Sequencing, Liquid Biopsies, and Patient-Derived Xenografts for Personalized Medicine in Melanoma. *Cancer Discovery.* **6**, 286-299 (2016).
36. Murphy, S.J. et al. Mate pair sequencing of whole-genome-amplified DNA following laser capture microdissection of prostate cancer. *DNA Research.* **19**, 395-406 (2012).
37. Smadbeck, J.B. et al. Copy number variant analysis using genome-wide mate-pair sequencing. *Genes Chromosomes and Cancer*. **57**, 459-470 (2018).
38. Kovtun, I.V. et al. Lineage relationship of Gleason patterns in Gleason score 7 prostate cancer. *Cancer Research.* **73**, 3275-3284 (2013).

656 39. Paster, E.V., Villines, K.A., Hickman, D.L. Endpoints for mouse abdominal tumor models:
657 refinement of current criteria. *Comparative Medicine.* **59**, 234–241 (2009).
658 40. Schneider, C.A., Rasband, W.S., Eliceiri, K.W. NIH Image to ImageJ: 25 years of image analysis.
659 *Nature Methods*. **9**, 671–675 (2012).
660 41. Cheng, Y. et al. MK-2206, a novel allosteric inhibitor of Akt, synergizes with gefitinib against
661 malignant glioma via modulating both autophagy and apoptosis. *Molecular Cancer Therapeutics*.
662 **11**, 154-164 (2012).
663 42. Rivera, V.M. et al. Ridaforolimus (AP23573; MK-8669), a potent mTOR inhibitor, has broad
664 antitumor activity and can be optimally administered using intermittent dosing regimens.
665 *Molecular Cancer Therapeutics.* **10**, 1059-1071 (2011).
666 43. Heitjan, D.F., Manni, A., Santen, R.J. Statistical analysis of in vivo tumor growth
667 experiments. *Cancer Research.* **53**, 6042–6050 (1993).
668 44. Vargas, R. et al. Case study: patient-derived clear cell adenocarcinoma xenograft model
669 longitudinally predicts treatment response. *NPJ Precision Oncology.* **2**, 14 (2018).
670 45. Harris, F.R. et al. Targeting HER2 in patient-derived xenograft ovarian cancer models
671 sensitizes tumors to chemotherapy. *Molecular Oncology*. **13**, 132-152 (2019).
672 46. Fidler, I.J. et al. Modulation of tumor cell response to chemotherapy by the organ
673 environment. *Cancer and Metastasis Reviews.* **13**, 209-222 (1994).
674

Figure 1

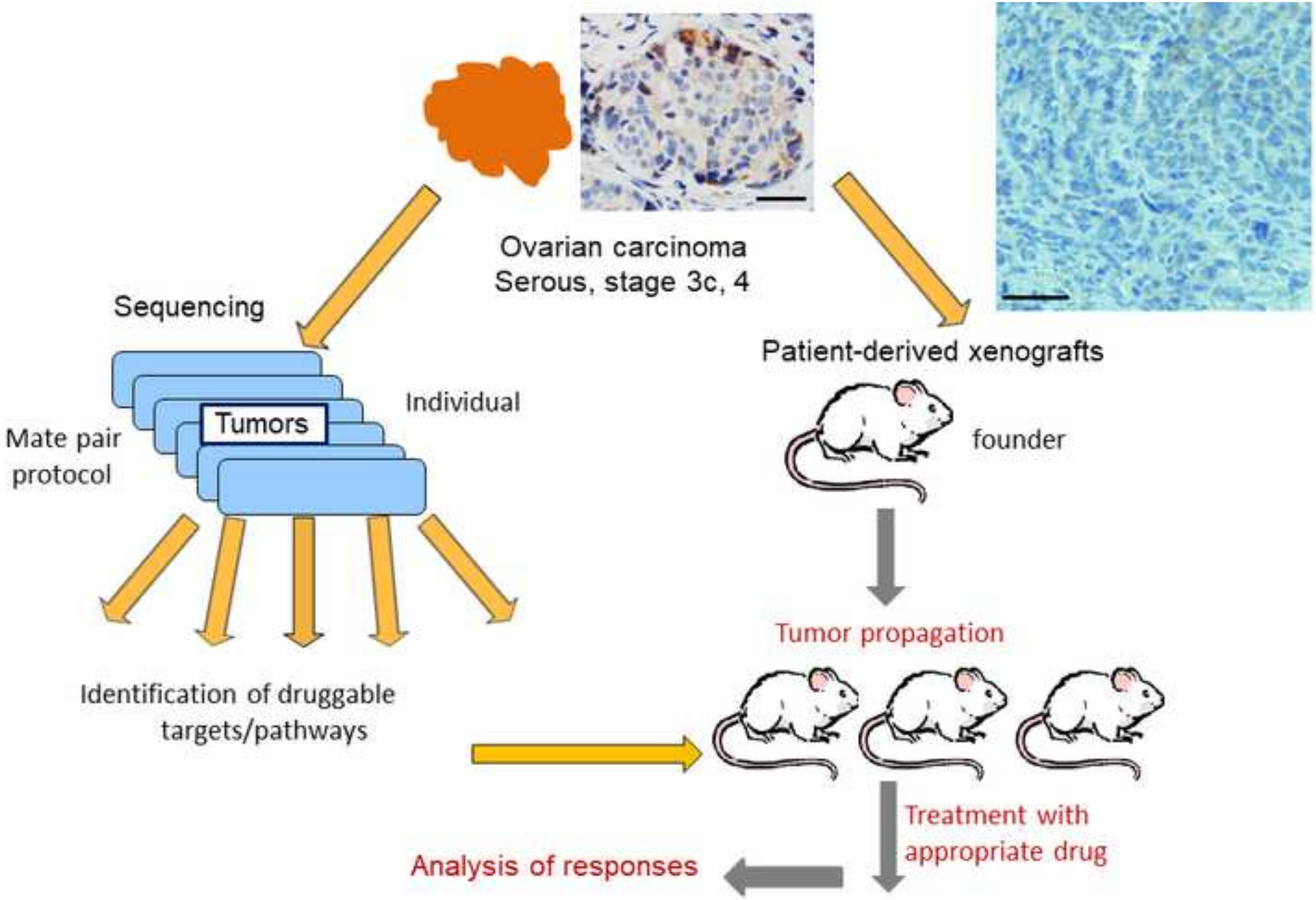

figure 2

Click here to access/download;Figure;Figure 2.tif

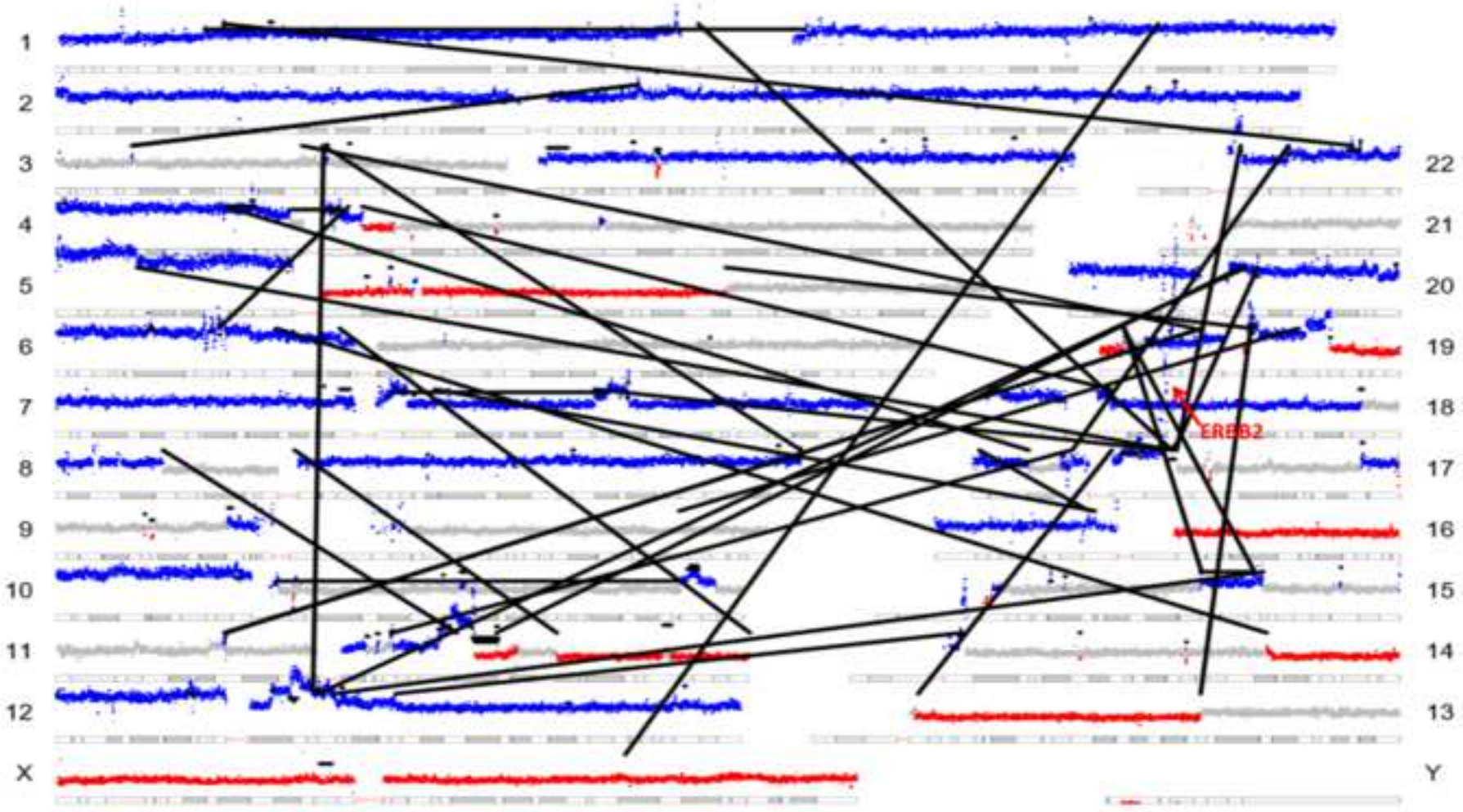

figure 3

Click here to access/download;Figure;Figure 3.tif

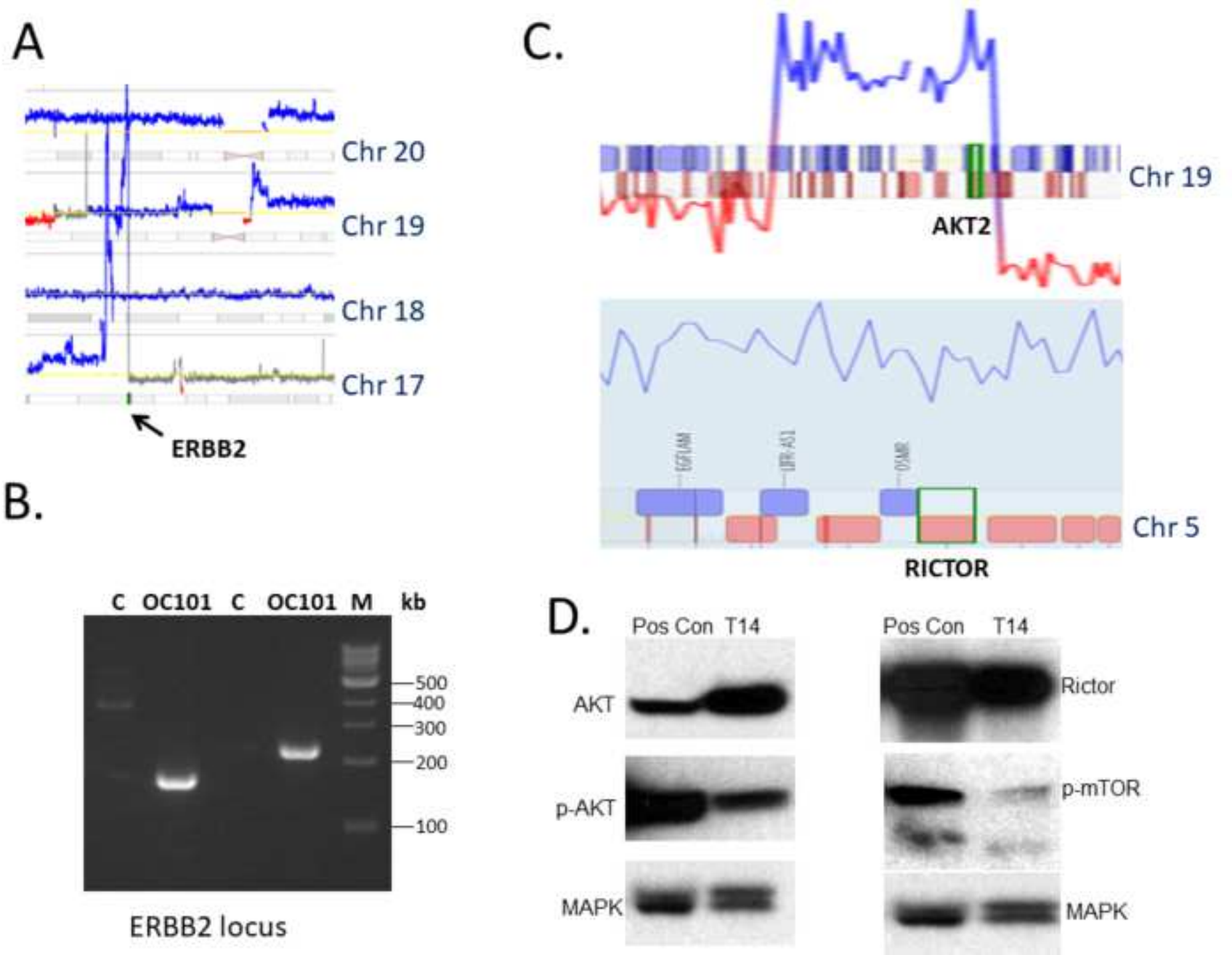

Figure 4

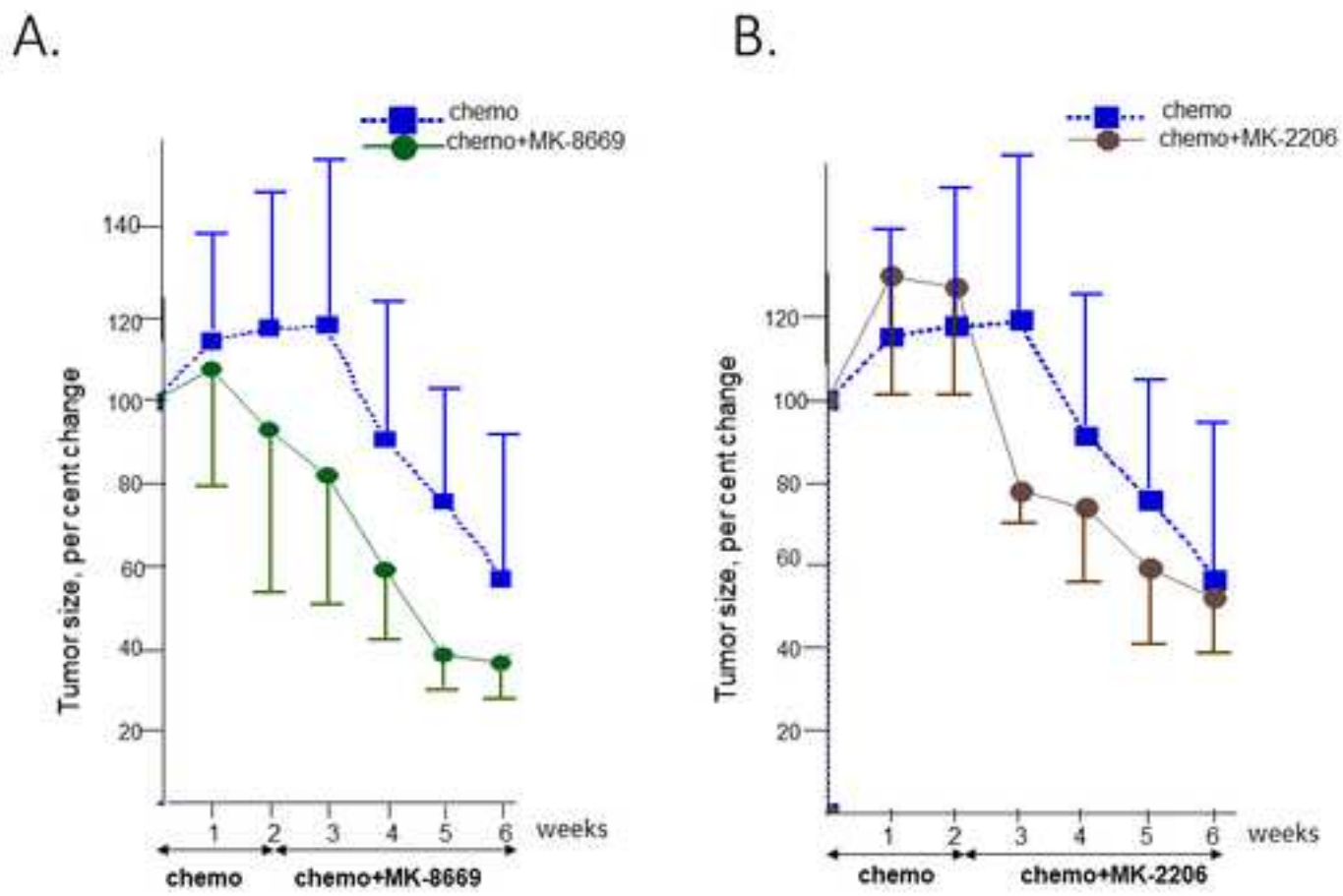

figure 5

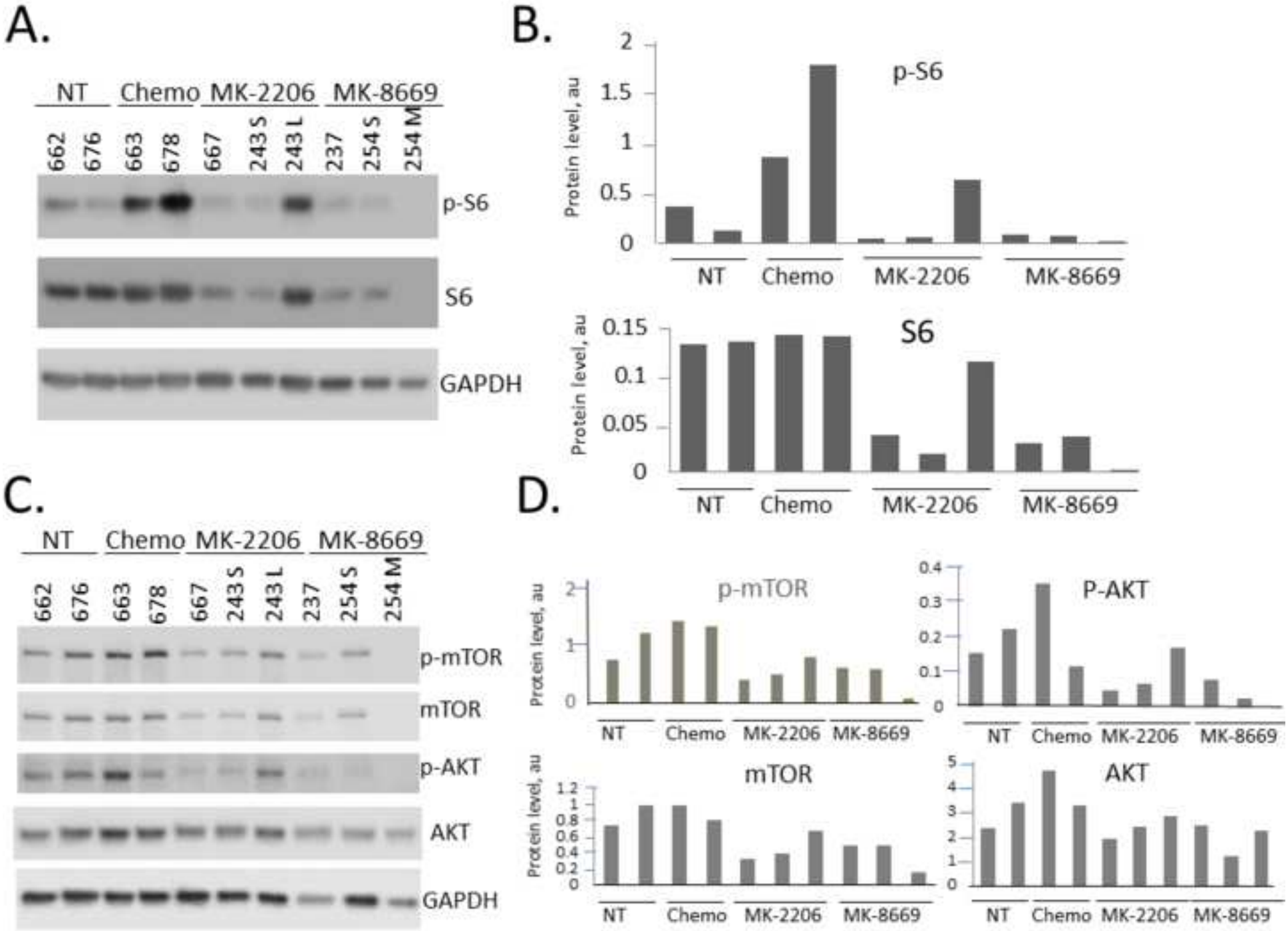

Table 1. Primers used for the validation of the OC101/17 alteration

Primer Name	Sequence	Primer Mix	Primers combined
OC101 17a-1	CTGGTCCTGGGAAATAGACACTAGATAAAT	1	OC101 F1 and R1
OC101 17a-1	GCTCAAGACAGTAACACCTAGTAGTTGATT	2	OC101 F1 and R2
OC101 17b-1	GGATTACGGGAACGTGCTACCTTG	3	OC101 F2 and R1
OC101 17b-1	AATGCCCTAGCAGTTCTATCCCCACTG	4	OC101 F2 and R2

Table 2. Setup for PCR to validate a junction.

Reagent	Quantity to add for 1 reaction (µL)	Quantity to add for 4 reactions (µL). [Multiply by 4.3 to make enough for each primer mix (4)]
Nuclease-free water	20.45	89.94
10x buffer (Easy A)	2.5	10.75
dNTPs 10 mM	0.5	2.15
Template DNA (concentration >10 ng/µL)	0.3	1.29
Taq Polymerase	0.25	1.08

Table 3. Cycling conditions for PCR to validate a junction.

Temp (C)	Time	
94	5 min	
94	40 s	35 cycles
59	40 s	
72	2 min	
72	5 min	
4	Hold	

Name of Material/ Equipment	Company
3M Vetbond	3M, Co.
anti-AKT antibody	Cell Signaling Technologie
Anti-GAPDH antibody(G-9)	Santa Cruz Biotech. Inc.
Anti-MAPK antibody	Cell Signaling Technologie
Anti-phospho-AKT antibody	Cell Signaling Technologie
Anti-mTOR antibody	Cell Signaling Technologie
Anti-Phospho-mTOR antibody	Cell Signaling Technologie
Anti-Phospho-S6 antibody	Cell Signaling Technologie
Anti-Rictor antibody	Cell Signaling Technologie
Anti-S6 antibody	Cell Signaling Technologie
Captisol	ChemScene, Inc.
Carboplatin	NOVAPLUS, Inc.
DMEM	Mediatech, Inc.
Easy-A Hi-Fi PCR Cloning Enzyme	Agilent, Inc.
Lubricant	Cardinal Healthcare
Matrigel	Corning, Inc.
McCoy's media	Mediatech, Inc.
MK-2206	ApexBio, Inc.
MK-8669	ARIAD Pharmaceuticals, Ir
Nair Sensitive Skin	Church & Dwight Co.
NOD/SCID mice	Charles River, Inc.

Paclitaxel	NOVAPLUS, Inc.
PEG400	Millipore Sigma, Inc.
Perjeta	Genetech, Co.
Rituximab	Genetech, Co.
RPMI1640	Mediatech, Inc.
SCID mice	Harlan Laboratories, Inc.
SLAx 13-6MHz linear transducer	FUJIFILM SonoSite, Inc
SonoSite S-series Ultrasound machine	FUJIFILM SonoSite, Inc
Tween 80	Millipore Sigma, Inc.

Catalog Number	Comments/Description
1469SB	
9272	
sc-365062	
9926	
9271	
2972	
2971	
4858	
2114	
2217	
cs-0731	
61703-360-18	
10-013-CV	
600404-51	
82-280	
356234	
10-050-CV	
A3010	
AP23573	
Nair Hair Remover Shower Power Sensitive	
NOD.CB17-*Prkdcscid* /NCrCrl	

55390-304-05

88440-250ML-F

Pertuzumab

Rituxan

10-040-CV

C.B.-17/IcrHsd-*Prkdc*^{scid} *Lyst*^{bg}

HFL38xp

SonoSite SII

P4780-100ML

June 3, 2020

To the Editor:

RE: JoVE60646

Dear Dr. Nguyen,

We have addressed the editorial comments in the text and in the video.

In the text, line 297 lists an action to anesthetize mice. The details of anesthesia are given in the line below,-299.

Thank you for your time and consideration

Sincerely,

Irina V. Kovtun, Ph.D
Assistant Professor
Department of Molecular Pharmacology
And Experimental Therapeutics
Mayo Clinic
Rochester, MN

507-250-0699
Email: ivkru@yahoo.com